Analysis of Shadow Contrast for Synthetic Aperture Sonar Imagery

Daniel A. Cook and Daniel C. Brown

***Abstract*—The contrast, or depth of shadows, in synthetic aperture sonar (SAS) imagery is arguably as important to image interpretation as the focus of the backscattered returns. The maximum contrast that can be achieved is determined by a combination of hardware, software, and environmental parameters. In this paper, the impact of these parameters on shadow contrast is quantified, and the contrast ratio is developed as a metric to predict a system's capacity to form imagery with well-defined shadows. A representative SAS is described, and its contrast ratio is investigated over a limited set of environmental and hardware parameters. This contrast ratio analysis can serve a tool for predicting system performance, determining the best dynamic range for display, and bounding the effects of manufacturing tolerances and motion errors.**

***Index Terms*—Synthetic aperture sonar, shadow, contrast, image quality**

I. Introduction

The interpretation of synthetic aperture sonar (SAS) imagery by humans relies on the shape and intensity of both the backscattered field from the scene and the shadows created by targets. Many automated target recognition (ATR) algorithms employ both parameters in their classification process [1], [2]. In order to obtain imagery that is useful for both ATR and humans, the system designer must consider many hardware and data processing design parameters to produce imagery that is well-focused with deep shadows and has the desired resolution.

The shadow contrast ratio is a metric that quantifies the shadow depth achievable relative to a bottom of a given scattering strength. The ultimate shadow contrast achieved within a SAS image can be limited by the hardware (transmitter and receiver dimensions, electronic noise floor, quantization noise, etc.), the software (motion estimation errors, beamforming approximations) or the environment (ambient noise, reverberation, multipath interference). Each of these can be controlled to some extent by the system design engineer. By studying the shadow contrast ratio, it is possible to balance system parameters to achieve a design that meets the specified contrast requirement.

II. Terrain to Shadow Contrast Ratio

Carrara et al. [3] describe the distributed target contrast ratio (DTCR) to quantify the ability to visually distinguish between two adjacent types of terrain, one having high backscatter and the other having low. The DTCR is defined as:

$$\begin{aligned}\mathrm{DTCR} &= \frac{\sigma_{0,\mathrm{high}} + \sigma_{\mathrm{n,total}}}{\sigma_{0,\mathrm{low}} + \sigma_{\mathrm{n,total}}} \\ &= \frac{\sigma_{0,\mathrm{high}} + \sigma_{\mathrm{n,add}} + \sigma_{\mathrm{n,mult}}}{\sigma_{0,\mathrm{low}} + \sigma_{\mathrm{n,add}} + \sigma_{\mathrm{n,mult}}} \\ &= \frac{\sigma_{0,\mathrm{high}} + \sigma_n + \mathrm{MNR}\ \bar{\sigma}_0}{\sigma_{0,\mathrm{low}} + \sigma_n + \mathrm{MNR}\ \bar{\sigma}_0}.\end{aligned} \tag{1}$$

TABLE I
Quantities contributing to DTCR.

$\sigma_{0,\mathrm{high}}$	Backscatter coefficient for brighter image region
$\sigma_{0,\mathrm{low}}$	Backscatter coefficient for darker image region
$\sigma_{\mathrm{n,total}}$	Equivalent backscatter coefficient of total noise
$\sigma_{\mathrm{n,add}}$	Equivalent backscatter coefficient of additive noise
$\sigma_{\mathrm{n,mult}}$	Equivalent backscatter coefficient of multiplicative noise
$\bar{\sigma}_0$	Average backscatter coefficient for sea floor
MNR	Multiplicative noise ratio

where the quantities used in this equation are given in Table I. The total noise $\sigma_{\mathrm{n,total}}$ is decomposed into $\sigma_{\mathrm{n,add}}$ and $\sigma_{\mathrm{n,mult}}$, which are the additive and multiplicative noise, respectively. The third line of Eq. (1) comes from [3] where common radar usage assumes that the most significant multiplicative noise sources can be combined into a single MNR value that is proportional to the average scene backscatter. Sonar must consider additional sources of multiplicative noise, namely volume and surface reverberation, so the sonar application begins with the second line of Eq. (1). As such, the multiplicative noise cannot be simplified and written as $\sigma_{\mathrm{n,mult}} = \mathrm{MNR}\ \bar{\sigma}_0$. The following sections describe the constituent sources of additive and multiplicative noise relevant to SAS.

A typical radar application for the DTCR might compare the (low) backscatter from a smooth asphalt road to the (high) backscatter from surrounding vegetated terrain. For SAS the low backscatter regions of interest are shadows, so $\sigma_{0,\mathrm{low}}$ is zero by definition. For notational simplicity the high backscatter region will be denoted simply as σ_0. This leads to the quantity sought; the terrain to shadow contrast ratio, or more simply, the contrast ratio (CR) of the image,

$$\mathrm{CR} = \frac{\sigma_0 + \sigma_{\mathrm{n,add}} + \sigma_{\mathrm{n,mult}}}{\sigma_{\mathrm{n,add}} + \sigma_{\mathrm{n,mult}}}. \tag{2}$$

The value of σ_0 is understood to represent the lowest backscatter in the scene which is to be distinguished from a shadow. In the absence of other requirements, the average sea floor backscatter for a given bottom type provides a reasonable value for σ_0. Note that the CR equation compares backscatter

Manuscript received July 30, 2010; revised August 8, 2010.

D. Cook is with the Sensors and Electromagnetic Applications Laboratory of the Georgia Tech Research Institute, Atlanta, GA. E-mail: dan.cook@gtri.gatech.edu

D. Brown is with the Sonar Research and Development Division of the Applied Research Laboratory, The Pennsylvania State University, State College, PA. E-mail: dcb19@psu.edu

cross-sections, so it is necessary to express the various noise contributions in these terms.

Two values of the contrast ratio are of particular interest. First, note that CR approaches 1 (0 dB) as the backscatter coefficient goes to zero. Depending on the bottom type, the CR can approach this case for grazing angles typical of long-range SAS imagery. A second interesting case occurs when the total noise contribution is equal to the bottom scattering, resulting in CR=2 (3 dB). The latter is a reasonable starting point for determining minimum contrast requirements.

III. Additive Noise

Additive noise is that form of noise that would be present in the recorded signal even with the transmitter deactivated. The two most significant contributions are system electronic noise and ambient sea noise:

$$\sigma_{\mathrm{n,add}} = \sigma_{\mathrm{self}} + \sigma_{\mathrm{ambient}}. \tag{3}$$

For a well-designed synthetic aperture sonar the system's self-noise is below the noise floor established by the ambient noise. At high frequencies the ambient noise is driven by thermal agitation of the water molecules, while at lower frequencies the ambient noise might be dominated by other natural or anthropogenic phenomena such as biologics, sea state, or shipping noise.

This analysis requires the additive noise to be expressed as an effective backscatter coefficient that may be derived from a signal-to-noise metric known to the radar community as the clutter-to-noise ratio (CNR): $\mathrm{CNR} = \sigma_0/\sigma_{\mathrm{n,add}}$. The clutter (desired signal) portion of CNR is the specific backscatter coefficient of the terrain of interest. The noise component is the thermal noise expressed as a specific backscatter coefficient, $\sigma_{\mathrm{n,add}}$ (or simply σ_{n}), which is also often called the noise-equivalent sigma zero (NESZ). It is the effective value of σ_0 that would produce a received signal equal in power to the system noise. Thus, the additive noise term needed for (2) is obtained by $\sigma_{\mathrm{n,add}} = \sigma_0/\mathrm{CNR}$.

The radar CNR relevant to SAR is found in several sources, for example [3]–[5]:

$$\mathrm{CNR}_{\mathrm{radar}} = \frac{1}{FkTB_{\mathrm{n}}} \cdot \frac{P_{\mathrm{TX}} G_{\mathrm{TX}} G_{\mathrm{RX}} \lambda^2 \sigma_0 \, \delta y \, \delta R_{\mathrm{g}}}{(4\pi)^3 r^4} \cdot \frac{2R\lambda N_{\mathrm{BT}}}{L_{\mathrm{eff}}^2}, \tag{4}$$

where the quantities used are defined in Table II. The first term in (4) represents the system's self noise, the second the signal power received by the radar, and the third the integration gain due to pulse compression in range and synthetic aperture processing in cross-range. To adapt this equation for SAS usage, all that is required is to replace the first term with the appropriate additive noise power, including both self-noise and ambient sea noise.

TABLE II
Variables used to compute the clutter-to-noise ratio.

F	System noise figure (dimensionless)
k	Boltzmann constant (1.38×10^{-23} J/K)
T	Temperature (K)
B_{n}	Noise bandwidth (Hz)
P_{TX}	Transmitted power (W)
G_{TX}	Transmit gain (dimensionless)
G_{RX}	Receive gain (dimensionless)
λ	Wavelength (m)
σ_0	Backscatter coefficient (dimensionless)
δy	Cross-range resolution (m)
δR_{g}	Range resolution in the ground plane (m)
R	Range (m)
N_{BT}	Time-bandwidth product (dimensionless)
L_{eff}	Effective antenna length (m)

IV. Multiplicative Noise

Multiplicative noise is so named because it rises and falls in proportion to the strength of the backscattered signal. It is independent of the transmitted signal power (i.e., doubling the transmitted power would double the multiplicative noise power). Sidelobes of the point scatterer response are a good example of a multiplicative noise source: Increasing the transmitted power increases both the mainlobe and the sidelobes by the same fraction.

Accoring to [3] the MNR is approximated by combining the primary sources of multiplicative noise, which are the range and along-track ambiguity ratio (ASR), the integrated sidelobe ratio (ISLR) of the image impulse response, and the quantization noise ratio (QNR). Application to sonar adds volume reverberation from the water column R_{vol} and the sea surface R_{surf}. These are combined as follows:

$$\sigma_{\mathrm{n,mult}} = \bar{\sigma}_0(\mathrm{ASR} + \mathrm{ISLR}) + \mathrm{QNR} + R_{\mathrm{surf}} + R_{\mathrm{vol}}, \tag{5}$$

where ASR and ISLR are proportional to the average sea floor backscatter. If surface and volume reverberation are negligible, then QNR is also proportional to $\bar{\sigma}_0$. Otherwise, it depends on the total backscattered intensity. The sources of multiplicative noise considered in this paper are described in Sections IV-A–IV-E below. Others can be found in Table 8.10 of [3].

Multipath is another source of multiplicative noise that must be considered for accurate estimation of the contrast for operation in littoral waters [6]. In this analysis, we focus on developing the contrast ratio for deeper water where multipath is safely ignored.

A. Ambiguity-to-Signal Ratio

The ambiguity to signal ratio (ASR) represents the superposition of along-track ambiguities (also called azimuth or Doppler ambiguities) and range ambiguities within the imaged scene. The primary assumption made is that all of the ambiguities are uncorrelated which allows their total contribution to be represented by a simple summation. Note that the ASR is a scale factor and has no reference quantity associated with its decibel representation.

The along-track ambiguities arise from the fact that the array elements are not spaced closely enough to avoid aliasing all spatial frequencies. A uniform linear array (ULA) consisting of omnidirectional elements must possess spacing finer than or equal to one-half wavelength in order to avoid spatial aliasing. SAS bypasses this constraint because the physical receivers are not omnidirectional. Their beampattern limits the range

of spatial frequencies that can impinge upon the array. Thus, the central portion of the mainlobe acts as a bandpass filter and the remaining beampattern determines the aliasing that occurs. Aliased returns manifest as multiplicative noise in the image, and the typical effect on the image is simply reduced contrast. However, highly-reflective discrete objects can cause visble 'ghosting' in the imagery (for example, see Figure 6.28 in [4]).

Viewed in this light, the spatial aliasing behavior is significant since the sinc function is generally considered to be a poor bandpass filter, yet it is typical of sonar beampatterns. Spatial aliasing can be controlled in several ways, such as increasing the along-track spatial sampling rate or by shaping the transmit and receive beampatterns.

Adding to the azimuth ambiguities are the range ambiguities, which are due to the echoes from earlier pings superimposed on the return from the current ping. Whereas the along-track ambiguities are attenuated by the composite transmit-receive directivity pattern, the range ambiguities are attenuated by spherical spreading losses and by absorption of acoustic energy in seawater.

The total ASR is given by the integral in Eq. (6), where $G = G_{\mathrm{TX}}G_{\mathrm{RX}}$ is the composite two-way transmit receive gain for a particular spatial frequency k_u (proportional to the angle from boresight for a broadside-looking sensor), σ_0 is the backscatter coefficient of the terrain, B_{p} is the processed spatial bandwidth, $k_{u\mathrm{s}}$ is the spatial sampling frequency in rad/m ($k_{u\mathrm{s}} = 2\pi/du$), du is the distance between along track samples (i.e., the phase center spacing), and f_{p} is the ping rate in Hz. The ASR is expressed as a function of time τ (or equivalently, range $R = c\tau/2$).

The radar literature frequently describes the along-track ambiguities in terms of Doppler frequency, rather than spatial frequency, as is done here. For broadside imaging the two are related by $f_{\mathrm{D}} = vk_u$, where v is the forward speed of the sensor. For a fixed temporal frequency, the spatial frequency is proportional to the angle of incidence across the array θ: $k_u = 2k\sin\theta$.

The processed bandwidth is the extent of the spectral region of support of the wavenumber k_u. Thus, the processed bandwidth is equivalent to an effective beamwidth. It is bounded above by the composite transmit-receive beamwidth, and it may be intentionally reduced in order to achieve better ASR performance. The cost of reducing B_{p} is a coarsening of the cross-range resolution of the image since narrowing the beam pattern shortens the synthetic aperture length. The resulting along-track resolution is given by $\delta y = 2\pi/B_{\mathrm{p}}$.

Interestingly, the processed spatial bandwidth has different meanings for spotlight and stripmap modes. The immediate concern is stripmap mode, for which the processed bandwidth is a measure of the cross-range resolution. In a spotlight SAR setting, the processed bandwidth indicates the width of the scene being imaged. The common thread is that processed bandwidth equates to narrowing the effective beamwidth. Thus, narrower beams reduce the length of the synthetic aperture in stripmap mode while they reduce the size of the illuminated scene in spotlight mode.

TABLE III
PROPERTIES OF COMMON 2D SPECTRAL WEIGHTING FUNCTIONS. THE MAINLOBE BROADENING FACTOR IS RELATIVE TO THE MAINLOBE WIDTH OF THE UNIFORM WINDOW (SINC) RESPONSE.

2D Window	ISLR (dB)	Mainlobe Broadening
Rectangular	-6.5	1
Taylor (5/35)	-24.6	1.32
Hamming	-31.3	1.46
Hanning	-29.9	1.56

B. Integrated Sidelobe Ratio

The integrated sidelobe ratio (ISLR) is the ratio of the energy in the sidelobes image impulse response to the energy in the mainlobe of the image impluse response. Here, the quantity of interest is the two-dimensional ISLR. Like the ASR, it is a scale factor and has no reference quantity associated with its decibel representation.

Under ideal conditions, the ISLR of the image impulse response is a function of the spectral support and weighting associated with the image reconstruction. However, errors due to miscalibration or motion can corrupt the impulse response causing the ISLR to deviate from the values given in Table III. The impact of phase errors on the impulse response is described in Chapter 5 of [3] and in [7].

C. Quantization Noise Ratio (QNR)

There are a number of models that can be used to describe quantization noise introduced by the analog-to-digital converter (ADC). The QNR of an ideal converter is $-(6.02N + 1.76)$ dB, where N is the number of bits; but it is rare in practice to achieve this level of performance [8]. Here, the simple rule of thumb found in [3] is used in which QNR is given by -5 dB per bit used in the ADC. This QNR is somewhat conservative relative to other measures. Like ASR and ISLR, the QNR is a scale factor and has no reference quantity associated with its decibel representation.

D. Reverberation

The total scattered field of sound waves propagating in the ocean environment is known as reverberation, and it is

$$\mathrm{ASR}(\tau) = \frac{\displaystyle\sum_{\substack{m,n=-\infty \\ m,n\neq 0}}^{\infty} \int_{-B_{\mathrm{p}}/2}^{-B_{\mathrm{p}}/2} G(k_u + mk_{u\mathrm{s}}, \tau + n/f_{\mathrm{p}}) \cdot \sigma_0(k_u + mk_{u\mathrm{s}}, \tau + n/f_{\mathrm{p}}) dk_u}{\displaystyle\int_{-B_{\mathrm{p}}/2}^{-B_{\mathrm{p}}/2} G(k_u, \tau) \cdot \sigma_0(k_u, \tau) dk_u} \tag{6}$$

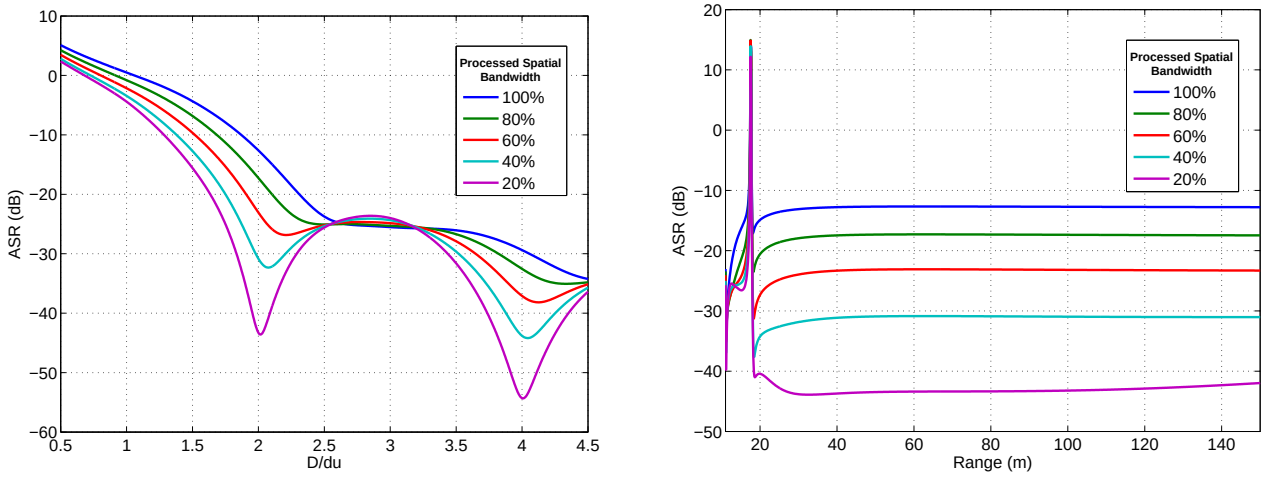

(a) Total ambiguity-to-signal ratio (ASR).

(b) Ambiguity-to-signal ratio as a function of range for the example configuration given in Table IV.

Fig. 1. Left: ASR at a fixed range, expressed as a function of normalized spatial sampling interval. Right: ASR as a function of range. The spikes correspond to the nulls in the vertical beampattern, where there is no bottom reflection to compete with the ambiguous reflections.

generally categorized as being associated with the sea floor, the sea surface, or a volume within the water column. In imaging applications, the bottom reverberation is the signal of interest (neglecting multipath effects), and the surface and volume reverberation are the multiplicative noise sources. The reverberation ratio (RR) is the fraction of energy received, attributable to reverberation, relative to what was transmitted into the water. Reverberation is highly dependent on the environment, making its impact on system performance sometimes difficult to represent accurately.

The analysis presented here in the context of SAS draws upon earlier work in the sonar and radar communities, emphasizing the themes common to both disciplines. The novel contributions introduced to address the ocean environment can be applied to SAR. Specifically, the phenomenon of volume reverberation can be used to model inhomogeneities in the ocean as well as weather effects such as rain falling on the scene being imaged by a SAR.

1) Volume Reverberation: Volume reverberation arises from the sound scattered from inhomogeneities within the water column. For a given range from the sonar, R, the portion of the water column that backscatters to produce volume reverberation is given by

$$V = \frac{c\tau_{\mathrm{p}}}{2}\Omega_{\mathrm{v}}R^2, \tag{7}$$

where τ_{p} is the pulse length, c is the speed of sound, and Ω_{v} is the solid angle subtended by the -3 dB level of the composite beampattern [9].

The volume reverberation ratio, $\mathrm{RR_v}$, is the ratio of the received volume-backscattered power to the transmitted power:

$$\mathrm{RR_v} = G_{\mathrm{TX}} \cdot \frac{A_{\mathrm{RX}} s_{\mathrm{v}} V}{(4\pi R^2)^2} \cdot \frac{1}{N_{\mathrm{BT}}} \cdot \frac{D^2}{2R\lambda}, \tag{8}$$

where s_{v} is the effective backscatter area per volume of water[1] ($\mathrm{m^2/m^3}$), and A_{R} is the effective area of each channel of the receive array ($\mathrm{m^2}$). The first term in (8), G_{TX}, is equivalent to the directivity index of the transmitter. In the second term, the product of the scattering area and receive area are normalized by the two-way spherical spreading. The last two terms in (8) are the reciprocal of the last term in (4). Here they represent the fact that pulse compression and synthetic aperture processing reduce reverberation ratio by diminishing the effective reverberating volume.

The contribution to the total multiplicative noise is found by multiplying s_{v} times the reverberating volume V which has been effectively reduced by the pulse compression and synthetic aperture processing gains:

$$\sigma_{\mathrm{vol}} = s_{\mathrm{v}} V \cdot \frac{1}{N_{\mathrm{BT}}} \cdot \frac{D^2}{2R\lambda}. \tag{9}$$

2) Surface Reverberation: Surface reverberation arises from the sound backscattered from the sea surface. This surface is assumed to be planar and the portion of the sea surface that backscatters at a given range R is given by

$$A = \frac{c\tau_{\mathrm{p}}}{2\sin\eta_i} R\theta_{\mathrm{s}}, \tag{10}$$

where η_i is the incidence angle and θ_{s} is the -3 dB composite horizontal beamwidth [9]. The surface reverberation ratio, $\mathrm{RR_s}$, is the ratio of the received surface-backscattered power to the transmitted power:

$$\mathrm{RR_s} = G_{\mathrm{TX}} \cdot \frac{A_{\mathrm{RX}} s_{\mathrm{s}} A}{(4\pi R^2)^2} \cdot \frac{1}{N_{\mathrm{BT}}} \cdot \frac{D^2}{2R\lambda}, \tag{11}$$

where s_{s} is the surface scattering strength per unit area ($\mathrm{m^2/m^2}$).

The contribution to the total multiplicative noise is found by multiplying s_{s} times the reverberating surface area A which

[1]The equivalent backscatter cross section for volume scattering is not dimensionless. When s_{v} reported in decibels, it is assumed to be normalized by 1 $\mathrm{m^2/m^3}$.

has been effectively reduced by the pulse compression and synthetic aperture processing gains:

$$\sigma_{\mathrm{surf}} = s_{\mathrm{s}} A \cdot \frac{1}{N_{\mathrm{BT}}} \cdot \frac{D^2}{2R\lambda}. \tag{12}$$

E. Medium Attentuation

For sonar, especially at frequencies used for imaging, it is critical to account for attentuation losses due to propagation through the medium. This effect can act strongly to counter the range ambiguities, and it is actually somewhat advantageous given the fact that SAS must operate under conditions where the receivers are operating virtually all of the time between transmitted pings. Medium attenuation is a less critical concern for radar, and it is typically ignored except in special situations such as the presence of falling rain between the radar and the imaged scene.

V. Discussion and Results

The interaction between the environment, the sonar system parameters, and the shadow contrast ratio is complicated. Beginning with image quality requirements (resolution and contrast) one can use the versatile framework provided here to guide many aspects of SAS system design and postprocessing. Nevertheless, it bears mentioning that what has been presented is an initial analysis, and that additional work can be done in order to get a better prediction of performance. For example, equations such as (4) used in this paper recognize the effect of the transmitted bandwidth. Meanwhile, the expression (6) for ASR assumes that the transmitted signal is effectively monochromatic. Although valid for narrowband systems, the ASR equation should be integrated over all temporal frequencies transmitted.

A. Image Formation Parameters and Contrast Ratio

Once data has been collected by a SAS many factors that determine the shadow contrast ratio are fixed. However, there are two components of the MNR that can be influenced by the image formation algorithm. The ISLR is determined in part by the selection of the spectral window applied to the data, summarized in Table III. The ASR is determined by the spatial sampling rate, which is set by the dimensions of the transmitter and receive array, and by the percentage of the available spatial bandwidth used to form imagery. In Fig. 1, the ASR is shown as a function of normalized spatial sampling rate for a variety of processed spatial bandwidths. The spatial sampling ratio is defined as D/du, where D is the width of the hydrophone implied by the horizontal beamwidth [10]. For values of the spatial sampling ratio (e.g., $D/du = 2$), a reduction of the processed bandwidth can greatly reduce the ASR.

Assuming either the ASR or ISLR dominate the noise terms that contribute to contrast loss, one can choose to reduce these ratios to improve shadow contrast; however, this action is not without cost. Reducing the ASR by reducing the spectral support used to form the image or improving the ISLR by spectral shaping will decrease the final image resolution. The specific requirements for resolution and contrast ratio must be weighed to determine the appropriate processing parameters.

TABLE IV
Parameters used in the analysis of the shadow contrast ratio.

Parameter	Value
Forward speed	$1.5\,\mathrm{m/s}$
Projector width	5 cm
Receiver width	5 cm
Projector height	2 cm
Receiver height	2 cm
Receiver spacing	5 cm
No. of receivers	16
Altitude	10 m
Water Depth	200 m
Max. range	150 m
Depression angle	10°
Center frequency	180 kHz
Bandwidth	30 kHz
Attenuation coeff.	$65.9\,\mathrm{dB/km}$
Transmit Level	220 dB re: $1\,\mu$Pa @ 1 m
σ_{self}	10 dB re: $1\,\mu\mathrm{Pa}^2/\mathrm{Hz}$ @ 1 m
$\sigma_{\mathrm{ambient}}$	30 dB re: $1\,\mu\mathrm{Pa}^2/\mathrm{Hz}$ @ 1 m
ISLR	-31.3 dB
QNR	-90 dBFS
θ_{s}	.15 rad
s_{s}	N/A (due to water depth)
Ω_{v}	.07 sr
s_{v}	-61 dB re: 1 m^{-1}

TABLE V
Equivalence between processed bandwidth, B_{p} and along-track resolution δy for the system described in Table IV. The Hanning window was used for spectral weighting.

B_{p} (%)	δ_y (cm)
100	3.9
80	4.9
60	6.5
40	9.8
20	19.5

B. Application to a Representative SAS Design

In this section, we investigate a small subset of the variables that contribute to the contrast ratio of a representative high-frequency SAS system. The parameters used are given in Table IV and they are based loosely on the SAS12 system developed under the sponsorship of the Office of Naval Research by the Naval Surface Warfare Center – Panama City Division and the Applied Research Laboratory at The Pennsylvania State University [12]. The beampatterns are assumed to be sinc functions, which depend only on the transducer dimensions and the wavelength. The example system transmits a band covering 165 kHz to 185 kHz and has a receive array that produces a spatial sampling rate of $D/du = 2$. This spatial sampling rate makes it possible to substantially decrease the ASR by processing reduced spatial bandwidth, as illustrated in Fig. 1. The cost of improving the contrast is coarsened resolution, as shown in Table V.

In Fig. 2, the shadow contrast ratio is plotted versus range for a pair of time-bandwidth products (N_{BT}=1 and N_{BT}=50) and for three bottom types (silt, medium sand, and rock). The

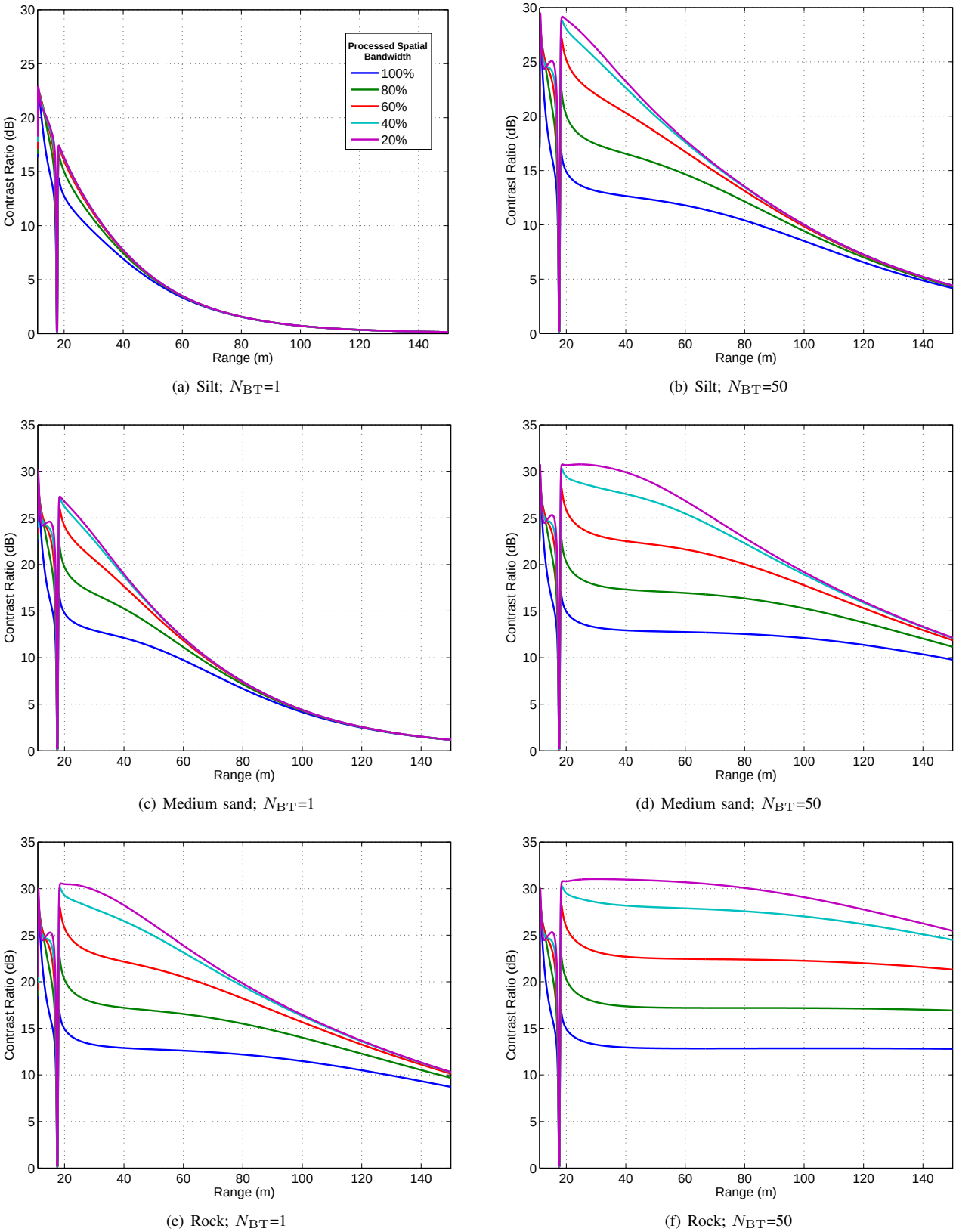

(a) Silt; N_{BT}=1

(b) Silt; N_{BT}=50

(c) Medium sand; N_{BT}=1

(d) Medium sand; N_{BT}=50

(e) Rock; N_{BT}=1

(f) Rock; N_{BT}=50

Fig. 2. Contrast ratio as a function of range plotted for various fractional processed bandwidths. The rows show representative bottom types (silt, medium sand, and rock), while the columns indicate the effect of the time-bandwidth product (N_{BT}=1 at left, N_{BT}=50 at right). The bottom scattering models used are given in Section IV-C of [11], and the system parameters used are given in Table IV. The legend contained in Fig. 2(a) applies to all of the plots on this page.

bottom backscattering strengths are evaluated as a function of grazing angle using an extrapolation of the values reported in [11]. The six examples shown in Figure 2 span a range of cases where the contrast ratio is limited by ambient noise at nearly all ranges, Fig. 2(a), to where the contrast ratio is limited by only multiplicative noise, Fig. 2(f). In the intermediate cases, the contrast ratio transitions from being limited by multiplicative noise sources at near range to additive noise sources at far ranges.

Against each bottom type, the contrast ratio is improved by increasing the time bandwidth product of the transmitted pulse; however, this gain is reduced at short ranges where multiplicative noise sources dominate. In each case, the contrast ratios asymptotically approach a value that is independent of the percentage of processed bandwidth. This indicates the range where the contrast ratio transitions from being limited by multiplicative noise to being limited by additive noise. For the N_{BT}=50 case, decreasing the processed bandwidth generally will improve the contrast ratio; however, against the silt bottom, these improvements are minimal beyond 100 m range.

C. Implications For SAS Hardware and Software Design

Many extant SAS systems have been developed for testing within the research and development (R&D) community. These systems have frequently been built with components that represented the state of the art at the time of their construction. They are typically built with transmitters that generate the maximum possible bandwidth and their receive arrays have high channel counts. While costly, this process has allowed R&D engineers to explore the limitations of SAS design and performance. SAS has recently begun to gain commercial and military acceptance [13], [14]. These systems must be designed to produce high quality imagery in a robust fashion, but they must also be sensitive to the cost of production.

A simple example of the cost/performance tradeoff can be found in the selection of the receiver element spacing, which determines the spatial sampling rate of a SAS receive array. The ASR for an array with $D/du = 2$ and 60% processed bandwidth is approximately the same as that for a $D/du = 2.5$ and 100% processed bandwidth. Assuming the shadow contrast is limited by the ASR, the CR will be the same for both systems. The $D/du = 2$ system will have 20% fewer receive channels, but its along-track resolution will be half that of the spatially oversampled system.

VI. Conclusion

A basic framework has been presented that can be used for SAS design performance prediction. It can also be used as a signal processing tool to predict and achieve optimum image quality relative to specified resolution and contrast requirements. The results show that contrast depends not only on system design, but also on the bottom composition. An important conclusion is that the environment can impose limits on the contrast ratio that are very difficult or even impossible to overcome. Such knowledge is useful because it offers a metric by which one can assess the sensor cost, giving an accurate representation of the image quality over the entire range swath as a function of sea floor type.

Acknowledgment

The authors are grateful to GTRI and ARL Penn State for allowing the informal collaboration that made this work possible.

References

[1] S. Reed, Y. Petillot, and J. Bell, "An automatic approach to the detection and extraction of mine features in sidescan sonar," *IEEE J. Ocean. Eng.*, vol. 28, no. 1, pp. 90 – 105, Jan. 2003.

[2] E. Dura, Y. Zhang, X. Liao, G. Dobeck, and L. Carin, "Active learning for detection of mine-like objects in side-scan sonar imagery," *IEEE J. Ocean. Eng.*, vol. 30, no. 2, pp. 360 – 371, Apr. 2005.

[3] W. G. Carrara, R. S. Goodman, and R. M. Majewski, *Spotlight Synthetic Aperture Radar Signal Processing Algorithms*. Artech House, 1995.

[4] J. C. Curlander and R. N. McDonough, *Synthetic Aperture Radar: Systems and Signal Processing*. John Wiley and Sons, Inc., 1991.

[5] M. A. Richards, J. A. Scheer, and W. A. Holm, Eds., *Principles of Modern Radar*. SciTech Publishing, Inc., 2010.

[6] A. Bellettini and M. Pinto, "Design and experimental results of a 300-khz synthetic aperture sonar optimized for shallow-water operations," *IEEE J. Ocean. Eng.*, vol. 34, no. 3, pp. 285–293, Jul. 2009.

[7] D. A. Cook and D. C. Brown, "Analysis of phase error effects on stripmap sas," *IEEE Journal of Oceanic Engineering*, vol. 34, no. 3, pp. 250–261, July 2009.

[8] H. Zumbahlen, Ed., *Linear Circuit Design Handbook*. Norwood, MA: Newnes, 2008.

[9] R. J. Urick, *Principles of Underwater Sound*, 3rd ed. Los Altos, CA: Peninsula Publishing, 1983.

[10] J. G. Mehlis, "Synthetic aperture radar range-azimuth ambiguity design and constraints," *IEEE International Radar Conference*, pp. 143–152, 1980.

[11] "APL-UW high-frequency ocean environmental acoustic models handbook," Applied Physics Laboratory - University of Washington, Seattle, WA, Tech. Rep. APL-UW TR 9407, Oct. 1994.

[12] A. D. Matthews, T. C. Montgomery, D. A. Cook, J. W. Oeschger, and J. S. Stroud, "12.75-inch synthetic aperture sonar (SAS), high resolution and automatic target recognition," in *MTS/IEEE Oceans 2006 Boston*, 2006.

[13] S. Wilcox, J. Bondaryk, K. Streitlein, C. Emblen, and J. Morrison, "A Bluefin-12 based system solution for the US Navy's Surface Mine Counter-Measures Unmanned Underwater Vehicle Program: Increment 2 (SMCM/UUV-2)," Bluefin Robotics Corporation, Tech. Rep., May 2003.

[14] R. Hansen, H. Callow, T. Saebo, P. Hagen, and B. Langli, "High fidelity synthetic aperture sonar products for target analysis," in *MTS/IEEE OCEANS Conf.*, Quebec, Sept. 2008, pp. 1–7.